Prevention and Epidemiology

Cancer Research

Diallyl Trisulfide Inhibits Phorbol Ester–Induced Tumor Promotion, Activation of AP-1, and Expression of COX-2 in Mouse Skin by Blocking JNK and Akt Signaling

Sangeeta Shrotriya[1], Joydeb Kumar Kundu[1], Hye-Kyung Na[4], and Young-Joon Surh[1,2,3]

Abstract

An inverse relationship exists between the consumption of garlic and the risk of certain cancers. The present study was aimed at investigating the effect of garlic constituent diallyl trisulfide (DATS) on 12-*O*-tetradecanoylphorbol-13-acetate (TPA)–induced cyclooxygenase-2 (COX-2) expression and tumor promotion in mouse skin and to explore the underlying molecular mechanisms. Pretreatment of mouse skin with different garlic-derived allyl sulfides showed DATS to be the most potent in suppressing TPA-induced COX-2 expression. DATS significantly attenuated the DNA binding of activator protein-1 (AP-1), one of the transcription factors that regulate COX-2 expression, in TPA-stimulated mouse skin. DATS also diminished TPA-induced expression of c-Jun and c-Fos, the principal components of AP-1, and blunted the activation of c-Jun NH_2-terminal kinase (JNK) and Akt. Pharmacologic inhibition of JNK or Akt by SP600125 or LY294002, respectively, resulted in diminished AP-1 DNA binding, reduced levels of c-Jun and c-Fos, and inhibition of COX-2 expression in TPA-treated mouse skin. The JNK or Akt kinase assay, taking c-Jun fusion protein as a substrate, revealed that TPA induced JNK- or Akt-mediated c-Jun phosphorylation in mouse skin, which was significantly attenuated by DATS or respective pharmacologic inhibitors. Evaluation of antitumor-promoting effect of DATS on 7,12-dimethylbenz(*a*)anthracene–initiated and TPA-promoted mouse skin carcinogenesis showed that pretreatment with DATS significantly reduced the incidence and multiplicity of papillomas. Taken together, the inhibitory effects of DATS on TPA-induced AP-1 activation and COX-2 expression through modulation of JNK or Akt signaling may partly account for its antitumor-promoting effect on mouse skin carcinogenesis. *Cancer Res; 70(5); 1932–40. ©2010 AACR.*

Introduction

A perilous loop exists between inflammation and cancer (1, 2). One of the well-defined molecular links between inflammation and cancer is the proinflammatory enzyme cyclooxygenase-2 (COX-2), which is a rate-limiting enzyme in the biosynthesis of prostaglandins (3). The levels of COX-2 are transiently elevated in cells or tissues stimulated with different growth factors, proinflammatory cytokines, endotoxin, and tumor promoters (4). COX-2 is aberrantly overexpressed in various premalignant and malignant tissues (4). Mice genetically engineered to overexpress *cox-2* are highly susceptible to spontaneous skin tumor formation (5), whereas *cox-2* knockout animals are less prone to develop chemically induced skin tumors (6). Selective COX-2 inhibitors have been shown to possess antitumor-promoting activities in different organ-specific cancers including that of skin (7). As evidenced by numerous epidemiologic and laboratory studies, targeted inhibition of COX-2 represents one of the most pragmatic approaches to prevent tumor promotion (3, 4).

Topical application of a prototype tumor promoter 12-*O*-tetradecanoylphorbol-13-acetate (TPA) induces the expression of COX-2 in mouse skin (8). Mechanistically, the expression of COX-2 in TPA-stimulated mouse skin involves excessive activation of intracellular signal transduction pathways comprising proline-directed serine/threonine kinases and their downstream transcription factors (4, 8–12). The 5′-flanking region of murine *cox-2* contains binding sites for various transcription factors, including NF-κB and activator protein-1 (AP-1; ref. 13). TPA has been shown to activate NF-κB (8, 10) and AP-1 (9, 14) in mouse skin through activation of mitogen-activated protein kinases (MAPK). Of the MAPK family members, extracellular signal-regulated kinase (ERK; ref. 8) and p38 MAPK (10) predominantly regulate the activation of NF-κB, whereas c-Jun NH_2-terminal kinase (JNK; ref. 14)

Authors' Affiliations: [1]National Research Laboratory of Molecular Carcinogenesis and Chemoprevention, College of Pharmacy, [2]Department of Molecular Medicine and Biopharmaceutical Sciences, Graduate School of Convergence Science and Technology, and [3]Cancer Research Institute, Seoul National University; [4]Department of Food and Nutrition, Sungshin Women's University, Seoul, South Korea

Note: Supplementary data for this article are available at Cancer Research Online (http://cancerres.aacrjournals.org/).

Current address for S. Shrotriya: Department of Pharmaceutical Sciences, University of Colorado School of Pharmacy, Aurora, CO 80045.

Corresponding Author: Young-Joon Surh, College of Pharmacy, Seoul National University, Shillim-dong, Kwanak-ku, Seoul 151-742, Korea. Phone: 82-2-880-7845; Fax: 82-2-874-9775; E-mail: surh@plaza.snu.ac.kr.

doi: 10.1158/0008-5472.CAN-09-3501

and p38 MAPK (9) regulate AP-1 DNA binding in TPA-treated mouse skin. TPA also phosphorylates another upstream kinase Akt, thereby leading to enhanced DNA binding of NF-κB and elevated expression of COX-2 in mouse skin (15). In the present study, we report that activated Akt also transmits signals to the downstream transcription factor AP-1 and regulates the subsequent expression of COX-2 in TPA-stimulated mouse skin.

One of the potential sources of chemopreventive phytochemicals is garlic, which contains organosulfur compounds, such as diallyl sulfide (DAS), diallyl disulfide (DADS), and diallyl trisulfide (DATS; refs. 16, 17). Among the garlic-derived allyl compounds, DATS is the most potent in suppressing constitutive expression of COX-2 in immortalized human embryonic kidney (HEK-293T) cells (18). Whereas DAS and DADS have been reported to inhibit chemically induced mouse skin tumor promotion (19), the anti-inflammatory and antitumor-promoting effects of DATS in mouse skin have not been investigated yet. Here, we report that topical application of DATS inhibits TPA-induced tumor promotion and COX-2 expression in mouse skin, which seemed to be mediated through blockade of AP-1 activation via downregulation of Akt and JNK signaling pathways.

Materials and Methods

Materials. DAS, DADS, and DATS (LKT Laboratories), TPA (Alexis Biochemicals), LY294002 and SP600125 (Tocris), and 7,12-dimethylbenz(*a*)anthracene (DMBA) and β-actin antibody (Sigma Chemical Co.) were purchased. Primary antibodies for IκBα, phospho-IκBα, ERK, p38 MAPK, JNK, c-Jun, p65, and purified glutathione *S*-transferase (GST)–c-Jun fusion protein were procured from Santa Cruz Biotechnology. COX-2 antibody was from Cayman Chemical Co. Akt and phospho-Akt antibodies were from Cell Signaling Technology. c-Fos antibody was obtained from Lab Vision. Lamin B antibody and horseradish peroxidase–conjugated anti-rabbit and anti-mouse secondary antibodies were purchased from Zymed Laboratories. Oligonucleotide probes containing NF-κB or AP-1 consensus sequence were acquired from Promega. Enhanced chemiluminescence detection kit and [γ-^{32}P]ATP were purchased from Amersham Pharmacia Biotech.

Animal treatment. Female ICR mice (6–7 wk) were supplied from Sankyo Laboservice Corp., Inc. and housed in climate-controlled quarters with a 12-h light/12-h dark cycle. DATS (5 or 25 μmol in 0.2 mL vehicle) and SP600125 (4 μmol in 0.2 mL vehicle) were applied topically to the shaved dorsal skin 30 min before TPA (10 nmol), whereas LY294002 (10 μmol in 0.2 mL vehicle) was cotreated with TPA. Control animals were treated with 10% DMSO in acetone. All experiments were performed using three animals per group.

Western blot analysis. Dorsal skins of mice treated with vehicle or TPA in the presence or absence of DATS, SP600125, or LY294002 were excised and fat was removed on ice. Collected epidermis was used to prepare whole tissue lysate, cytosolic, and nuclear protein extracts as described (11). Protein samples were separated by SDS-PAGE and immunoblot analysis was performed according to the procedure described earlier (11). Immunoblot membranes were incubated for 4 h at room temperature with 1:1,000 dilution of primary antibodies for COX-2, Akt, and JNK and for 12 h at 4°C with 1:1,000 dilution of primary antibodies for lamin B, p65, phospho-JNK, phospho-Akt, c-Jun, and c-Fos. Immunoblots were then probed with horseradish peroxidase–conjugated rabbit or mouse secondary antibodies for 1 h and visualized according to the procedure described previously (11).

Immunohistochemical staining. Sections (4 μm) of 10% formalin-fixed, paraffin-embedded skin tissues from mice (n = 3 per group) treated with vehicle or TPA in the presence or absence of DATS (25 μmol), SP600125 (4 μmol), or LY294002 (10 μmol) were subjected to immunohistochemical analysis for detecting the epidermal expression of COX-2, phospho-JNK, c-Jun, and c-Fos following the procedure described earlier (11). The quantification of immunohistochemical data was achieved by counting the positively stained cells as percent of total epidermal cells from 10 microscopic fields of immunostained tissues.

Electrophoretic mobility shift assay. Epidermal nuclear extracts were prepared from mice treated with vehicle or TPA in the presence or absence of DATS, SP600125, or LY294002 for 2 h. Oligonucleotides for NF-κB (5′-GAGGGGATTCCCTTA-3′) and AP-1 (5′-CGCTTGATGAGTCAGCCGGAAC-3′) were labeled with [γ-^{32}P]ATP and incubated with nuclear proteins from different treatment groups. The DNA binding of NF-κB and AP-1 was assessed by electrophoretic mobility shift assay (EMSA) as described (11).

In vitro *radioactive kinase assay.* The catalytic activities of JNK and Akt in mouse skin treated with TPA for 2 h in the presence or absence of DATS, SP600125, or LY294002 were examined by *in vitro* kinase assay using GST–c-Jun as the substrate protein for both JNK and Akt following the protocol described previously (11). Briefly, epidermal extract (200 μg) was immunoprecipitated with Akt (for Akt kinase assay) or JNK (for JNK kinase assay) antibody. The immunoprecipitate was suspended in 50 μL of reaction mix containing 47 μL of 1× kinase buffer, 1 μg of GST–c-Jun fusion protein, and 10 μCi [γ-^{32}P]ATP and incubated at 30°C for 45 min. The kinase reaction was stopped by adding 2.5× SDS loading dye, boiled at 99°C for 5 min, and centrifuged at 5000 rpm for 2 min. The supernatant was separated by gel electrophoresis followed by gel staining and destaining as described (11). The destained gel was dried and exposed to X-ray film to detect the phosphorylated GST–c-Jun in the autoradiogram.

Two-stage mouse skin carcinogenesis. Female ICR mice were randomly divided into five groups, each consisting of 18 animals. Mice from groups II, III, and IV were treated on their shaven backs with single topical application of DMBA (0.2 μmol) dissolved in 0.2 mL of acetone/DMSO (85:15, v/v) and animals in groups I and V were treated only with vehicle. One week after initiation with DMBA, animals in groups II, III, and IV were treated topically with TPA (10 nmol) twice a week for 20 wk. DATS was applied topically at doses of 5 and 25 μmol 30 min before each TPA treatment to animals in groups III and IV, respectively, until the termination of experiment at 20th

week. Animals in groups I and V were treated with vehicle alone and DATS (25 μmol), respectively, twice a week for 20 wk. Tumors of at least 1 mm diameter were counted every week until 20 wk.

Statistical analyses. Values were expressed as the mean ± SEM of at least three independent experiments. The intensity of different immunoblots was measured by using Gel-Pro image density analyzer, and statistical analysis was performed by using Microsoft Excel.

Results

Topically applied DATS inhibited TPA-induced COX-2 expression in mouse skin. As an initial approach, the relative potency of DAS, DADS, and DATS (25 μmol each) in suppressing COX-2 expression in TPA-treated mouse skin was evaluated. Pretreatment with DADS or DATS, but not DAS, significantly attenuated TPA-induced expression of COX-2. DATS was found to be more potent than DADS (Fig. 1A), and its effect was dose dependent (Fig. 1B). Immunohistochemical analysis (Fig. 1C) verified the pronounced inhibitory effect of DATS on TPA-induced COX-2 expression. Thus, DATS significantly reduced the epidermal COX-2 positivity compared with TPA treatment alone (Fig. 1D). DATS alone had no effect on COX-2 induction in mouse skin.

DATS attenuated TPA-induced activation of AP-1 in mouse skin. One of the major transcription factors that regulate the expression of COX-2 is AP-1, which on activation bind to the 5′-flanking region of *cox-2* gene promoter (13, 20). Pretreatment with DATS negated the AP-1 DNA binding (Fig. 2A) in TPA-stimulated mouse skin. DATS also diminished TPA-induced expression of c-Jun and c-Fos in mouse skin as determined by immunoblot (Fig. 2B) as well as immunohistochemical analyses (Fig. 2C).

TPA-induced activation of JNK was abrogated by DATS in mouse skin. The activation of AP-1 in TPA-treated mouse skin often involves amplification of signaling mediated through upstream p38 MAPK (9) and JNK (14). Although pretreatment with DATS significantly attenuated the phosphorylation of JNK (Fig. 3A), it barely affected the phosphorylation of p38 MAPK (data not shown) in TPA-treated mouse skin. The inhibitory effect of DATS on TPA-induced phosphorylation of JNK

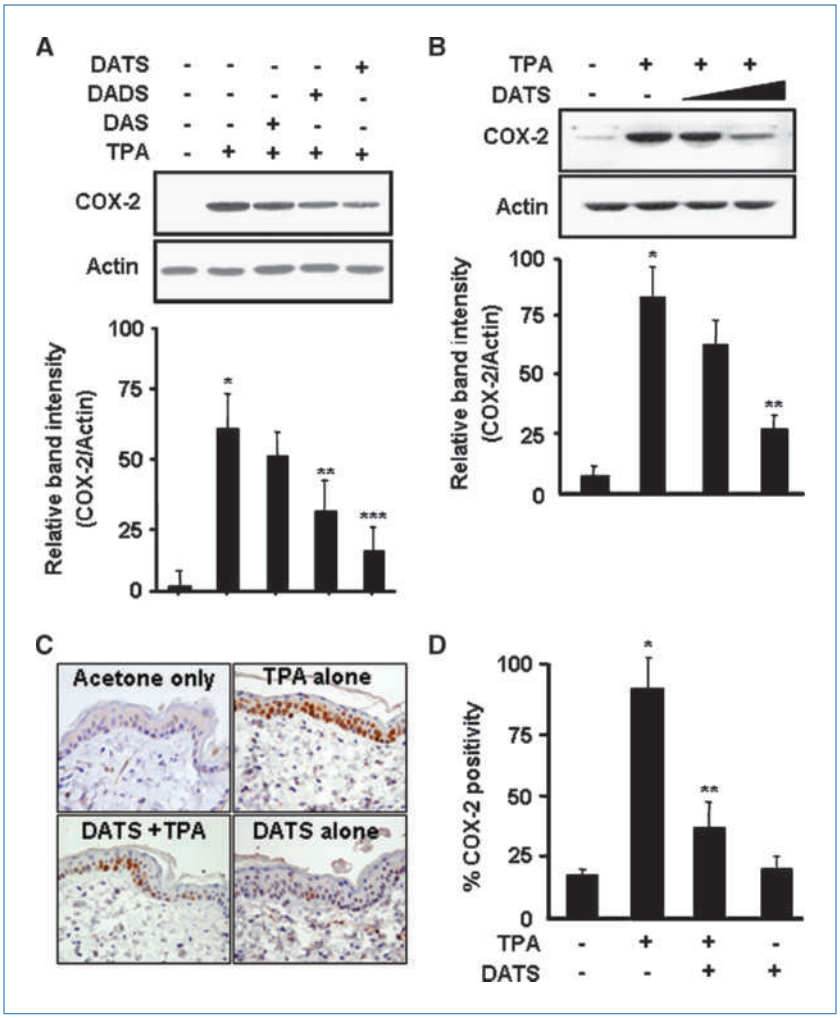

Figure 1. Inhibitory effect of DATS on TPA-induced COX-2 expression in mouse skin. A, dorsal skins of mice (n = 3 per group) were treated topically with 25 μmol each of DAS, DADS, or DATS dissolved in 0.2 mL vehicle (acetone/DMSO, 90:10, v/v) 30 min before application of TPA (10 nmol in 0.2 mL acetone). Control animals (n = 3) were treated with the vehicle in lieu of TPA. Animals were sacrificed 4 h later. Epidermal lysates were analyzed for COX-2 expression by immunoblotting. *, $P < 0.001$ (control versus TPA); **, $P < 0.05$ (TPA versus DADS plus TPA); ***, $P < 0.001$ (TPA versus DATS plus TPA). Mice (n = 3 per group) were treated on their shaven backs with vehicle or DATS (5 or 25 μmol) 30 min before TPA treatment and sacrificed after 4 h. Epidermal COX-2 expression was examined by Western blotting (B) and immunohistochemistry (C). Representative photomicrograph (magnification at ×400) illustrating epidermal COX-2 expression. *, $P < 0.001$ (control versus TPA); **, $P < 0.001$ (TPA versus 25 μmol DATS plus TPA). D, epidermal COX-2 positivity was calculated from 10 equal sections of immunostained tissues from each animal. *, $P < 0.001$ (control versus TPA); **, $P < 0.001$ (TPA versus 25 μmol DATS plus TPA).

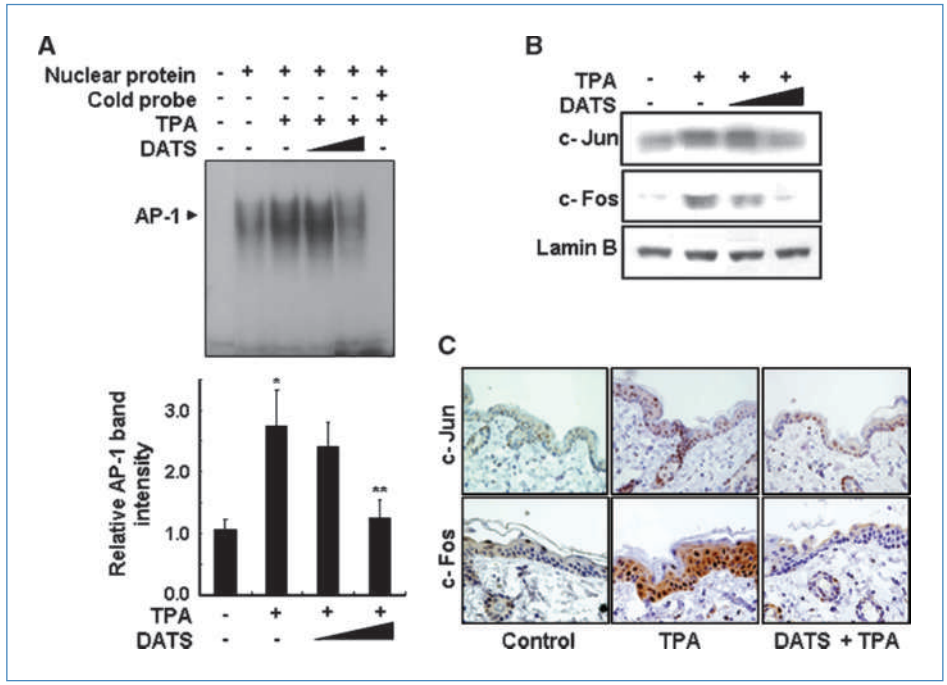

Figure 2. Effects of DATS on TPA-induced activation of AP-1 in mouse skin. Animals were treated as described in Fig. 1B and sacrificed after 2 h of TPA treatment. Nuclear extracts were analyzed by the EMSA. A, effects of DATS on TPA-induced AP-1 DNA binding. Representative data showing probe only (lane 1), vehicle control (lane 2), TPA alone (lane 3), 5 μmol DATS plus TPA (lane 4), 25 μmol DATS plus TPA (lane 5), and nuclear extract from TPA-treated skin plus 100-fold excess unlabeled AP-1 oligonucleotide (lane 6). *, $P < 0.001$ (vehicle only versus TPA alone); **, $P < 0.001$ (TPA versus 25 μmol DATS plus TPA). Nuclear extracts were subjected to Western blot analysis (B) and immunohistochemistry (C) to determine the expression of c-Jun and c-Fos. Data are representative of three independent experiments. Right, representative photomicrograph (magnification ×400) showing epidermal expression of c-Jun and c-Fos.

was further confirmed by immunohistochemical analysis. As shown in Fig. 3B, pretreatment with DATS significantly diminished TPA-induced phosphorylation of JNK in comparison with TPA treatment alone. Assessment of JNK activity by an *in vitro* JNK kinase assay using GST–c-Jun fusion protein as a substrate showed that TPA enhanced the catalytic activity of JNK in mouse skin, which was significantly attenuated by pretreatment with DATS (Fig. 3C).

JNK is involved in TPA-induced activation of AP-1 and expression of COX-2 in mouse skin. To examine the role of JNK in TPA-induced activation of AP-1 and expression of COX-2 in mouse skin, we used the pharmacologic inhibitor (SP600125) of JNK. Pretreatment with a topical dose (4 μmol) of SP600125 abrogated TPA-induced phosphorylation of JNK as assessed by immunoblot (Fig. 4A, left) and immunohistochemical analyses (Fig. 4A, right). Likewise,

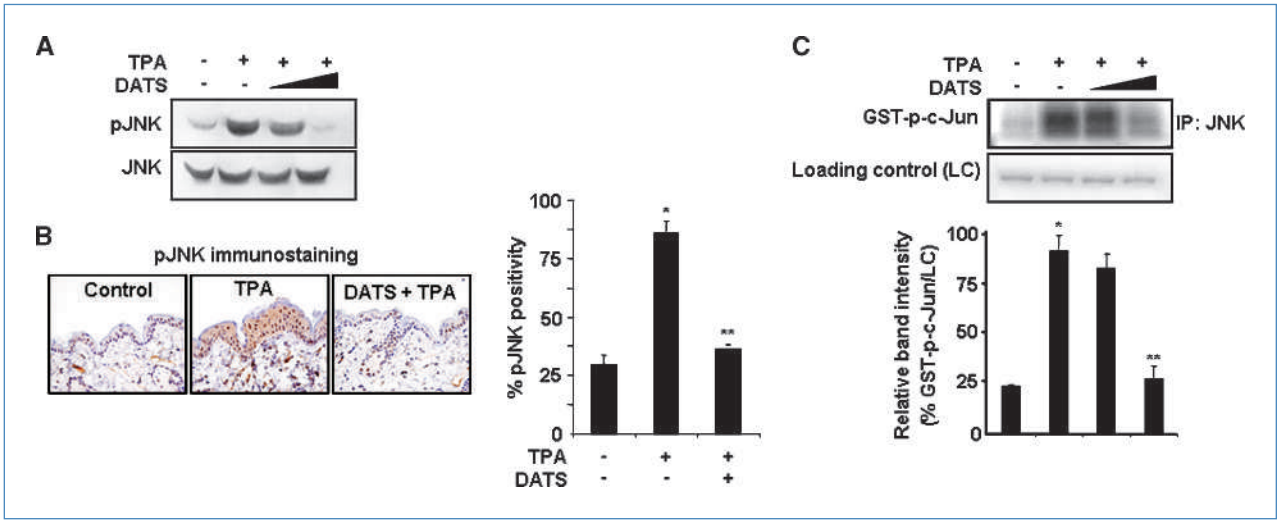

Figure 3. Inhibitory effect of DATS on TPA-induced activation of JNK in mouse skin. Epidermal extract was prepared from mice treated as described in Fig. 1B and sacrificed after 2 h of TPA application. A, representative data showing the inhibitory effect of DATS on TPA-induced phosphorylation of JNK. B, left, representative photomicrograph (magnification ×40) showing epidermal phospho-JNK (pJNK)–positive cells as stained brown color. Percent epidermal phospho-JNK positivity in different treatment groups was calculated by analyzing 10 equal sections of immunostained tissues from each animal. *, $P < 0.05$ (control versus TPA alone); **, $P < 0.05$ (TPA versus 25 μmol DATS plus TPA). C, epidermal extracts were subjected to the JNK activity assay as described in Materials and Methods. *, $P < 0.001$ (control versus TPA alone); **, $P < 0.001$ (TPA versus 25 μmol DATS plus TPA).

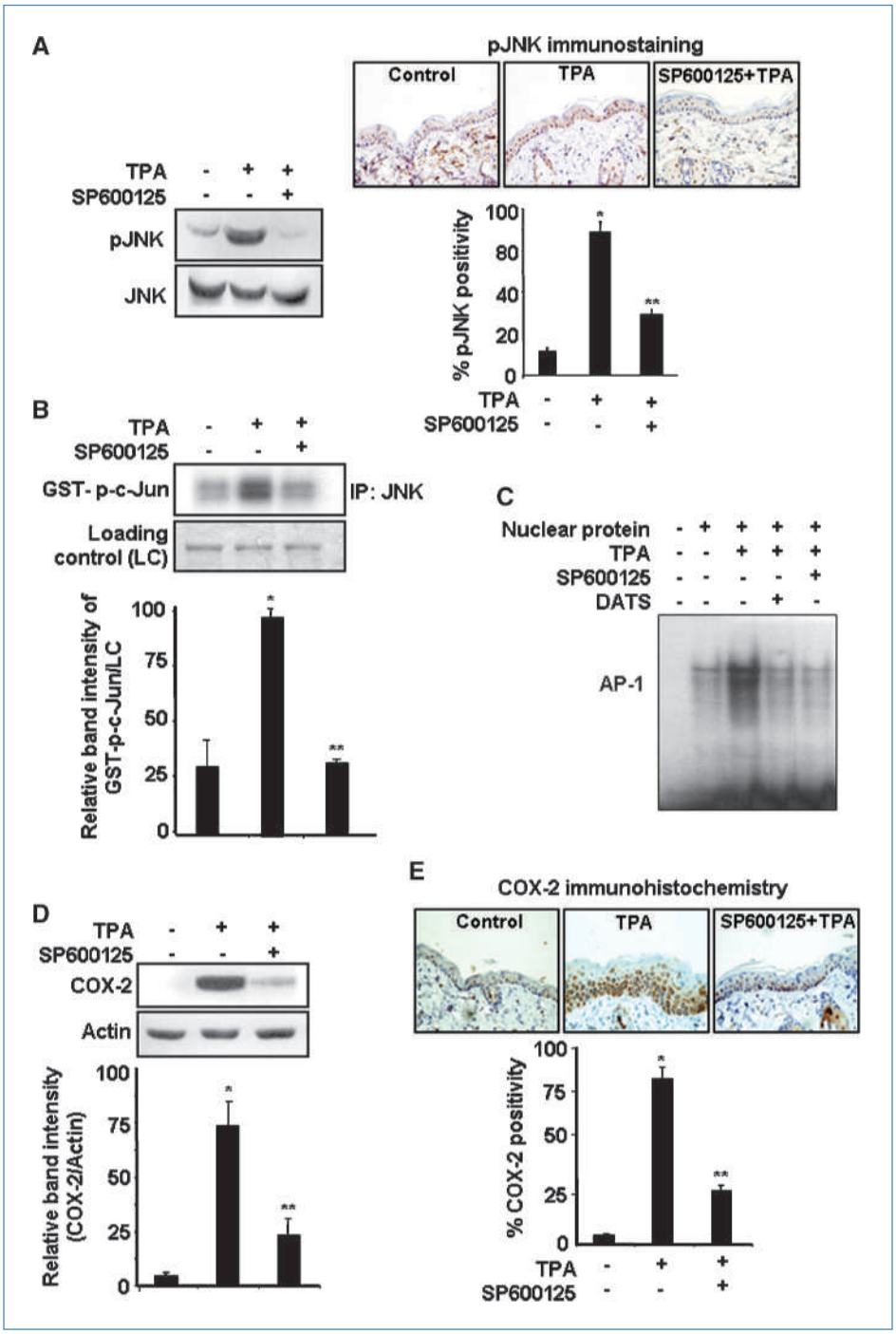

Figure 4. Effects of SP600125 on TPA-induced activation of JNK, DNA binding of AP-1, and expression of COX-2 in mouse skin. Mice ($n = 3$ per group) were treated on their shaven backs with vehicle, DATS (25 μmol), or SP600125 (4 μmol) 30 min before TPA application and sacrificed after 2 or 4 h. A, epidermal lysates or formalin-fixed skin tissues prepared after 2 h of TPA treatment were subjected to immunoblot (left) or immunohistochemical analysis (right) to examine the expression of phospho-JNK. Data are representative of three independent experiments. Right, percent phospho-JNK positivity. *, $P < 0.001$ (solvent control versus TPA alone); **, $P < 0.05$ (TPA versus SP600125 plus TPA). B, the *in vitro* JNK activity assay was performed with epidermal lysate from mice treated with TPA for 2 h in the presence or absence of SP600125. *, $P < 0.05$ (control versus TPA alone); **, $P < 0.05$ (TPA versus SP600125 plus TPA). C, epidermal nuclear extracts (2 h after TPA treatment) from mice treated as above were analyzed by EMSA to examine the AP-1 DNA binding. Data are representative of three independent experiments. D and E, total epidermal lysates or formalin-fixed skin tissues prepared from animals treated as described above and sacrificed at 4 h after TPA application were examined for epidermal COX-2 expression by immunoblotting (D; *, $P < 0.001$, control versus TPA alone; **, $P < 0.001$, TPA versus SP600125 plus TPA) or by immunohistochemical analysis (E; *, $P < 0.001$, control versus TPA alone; **, $P < 0.05$, TPA versus SP600125 plus TPA).

SP600125 significantly attenuated TPA-induced JNK activity in mouse skin (Fig. 4B). We attempted to explore a mechanistic link between JNK and the transcription factor AP-1 with regard to upregulation of COX-2 expression in TPA-treated mouse skin. As shown in Fig. 4C, topical application of SP600125 negated TPA-induced DNA binding of AP-1. Moreover, the immunoblot (Fig. 4D) and immunohistochemical (Fig. 4E) analyses revealed that the inactivation of JNK with SP600125 significantly inhibited TPA-induced COX-2 expression in mouse skin.

DATS inhibited TPA-induced activation of AP-1 and expression of COX-2 in mouse skin by blocking Akt signaling. TPA-induced expression of COX-2 in mouse skin is regulated by upstream kinase Akt (15). Pretreatment with DATS inhibited TPA-induced phosphorylation of Akt in a dose-dependent manner (Fig. 5A, left; Supplementary

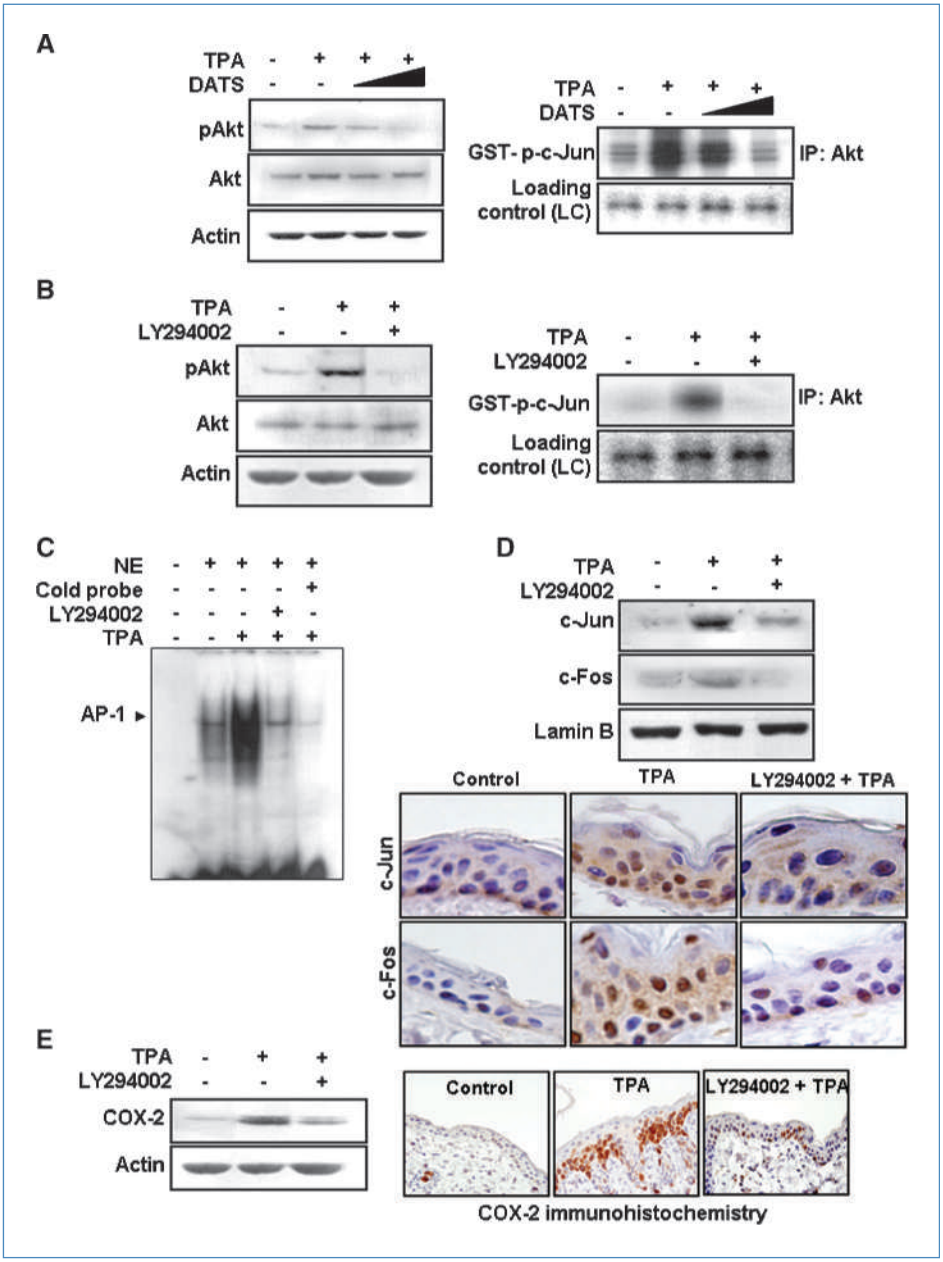

Figure 5. Role of Akt in TPA-induced activation of AP-1 and expression of COX-2 in mouse skin and its modulation by DATS. Mice (n = 3 per group) were treated with DATS (5 or 25 μmol) or LY294002 (10 μmol) 30 min before or along with TPA, respectively, and animals were sacrificed 2 or 4 h later. Control animals were treated with vehicle alone. A, epidermal lysates from mice treated with TPA for 2 h with or without DATS were subjected to (left) immunoblot analysis with phospho-Akt antibody (*, $P < 0.001$, control versus TPA alone; **, $P < 0.001$, 25 μmol DATS plus TPA versus TPA alone; Supplementary Fig. S1A) and the (right) Akt kinase assay using GST–c-Jun as a substrate protein (*, $P < 0.05$, control versus TPA alone; **, $P < 0.05$, 25 μmol DATS plus TPA versus TPA alone; Supplementary Fig. S1B). B, lysates from mouse skin treated with TPA for 2 h in the presence or absence of LY294002 were subjected to Western blot analysis to detect the expression of phospho-Akt (left; data are representative of three independent experiments) and the Akt kinase activity assay (right). *, $P < 0.05$, control versus TPA alone; **, $P < 0.05$, TPA versus LY294002 plus TPA (Supplementary Fig. S1C). C, epidermal nuclear protein (10 μg) prepared 2 h after TPA treatment in the presence or absence of LY294002 was subjected to analysis by EMSA for assessing the AP-1 DNA binding. Lane 1, free probe only; lane 2, acetone control; lane 3, TPA alone; lane 4, LY294002 plus TPA; lane 5, nuclear protein plus 100-fold excess unlabeled AP-1 oligonucleotide. D, epidermal tissue lysates or formalin-fixed skin tissue from mice treated with TPA for 2 h in the presence or absence of LY294002 was subjected to immunoblot (top; data are representative of three independent experiments) or immunohistochemical analysis (bottom) to examine the expression of c-Jun and c-Fos. E, total epidermal lysates or formalin-fixed skin tissues prepared from animals treated with TPA for 4 h in the presence or absence of LY294002 were examined for epidermal COX-2 expression by (D) immunoblotting (*, $P < 0.001$, control versus TPA alone; **, $P < 0.001$, TPA versus LY294002 plus TPA; Supplementary Fig. S1D) or by (E) immunohistochemical analysis (*, $P < 0.001$, control versus TPA alone; **, $P < 0.05$, TPA versus LY294002 plus TPA; Supplementary Fig. S1E).

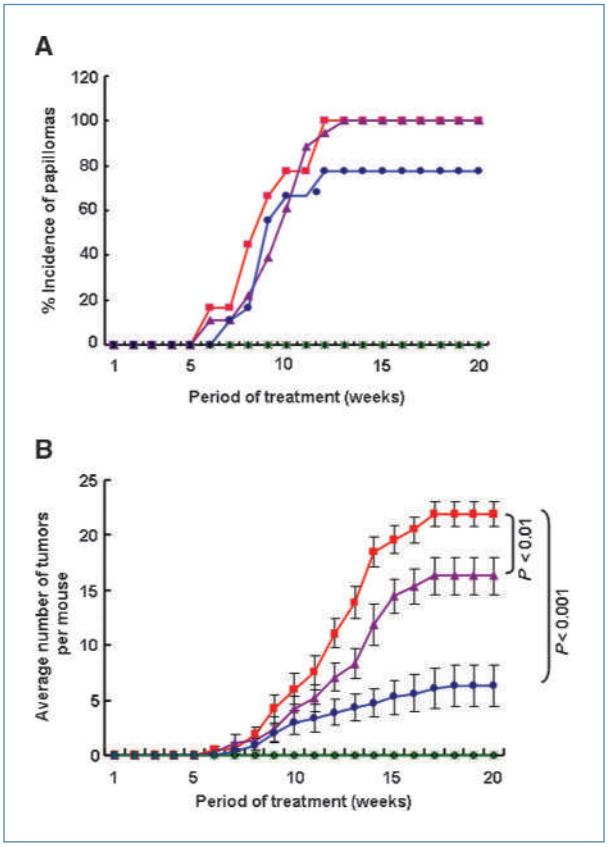

Figure 6. Inhibitory effects of DATS on DMBA-initiated and TPA-promoted mouse skin papillomagenesis. Female ICR mice (n = 18 per group) were first treated with DMBA (0.2 μmol), except those in group that served as control group and that treated with DATS alone. After 1 wk of DMBA initiation, animals were treated with vehicle or DATS (5 or 25 μmol) 30 min before each topical application of TPA (10 nmol) twice a week for 20 wk. Treatment groups: (♦) vehicle only, (■) DMBA plus TPA, (▲) DMBA plus DATS (5 μmol) plus TPA, (●) DMBA plus DATS (25 μmol) plus TPA, (*) DATS (25 μmol) alone. A, percent incidence of papillomas. B, average numbers of papillomas per mouse in different treatment groups. The average numbers of papillomas per mouse at the 20th week were found to be 16.28 ± 1.64 and 6.33 ± 1.88 in groups treated with DATS at doses of 5 and 25 μmol, respectively, which were significantly less than that observed in animals treated only with DMBA plus TPA (21.89 ± 1.16).

Fig. S1A). The *in vitro* Akt kinase assay revealed that DATS pretreatment also attenuated TPA-induced Akt activity by reducing the phosphorylation of the target substrate GST–c-Jun (Fig. 5A, right; Supplementary Fig. S1B). Likewise, topical application of LY294002, a pharmacologic inhibitor of Akt, abrogated TPA-induced phosphorylation (Fig. 5B, left) and the activity (Fig. 5B, right; Supplementary Fig. S1C) of Akt in mouse skin. Furthermore, topically applied LY294002 significantly attenuated TPA-induced DNA binding of AP-1 in mouse skin (Fig. 5C). In addition, the expression of c-Jun and c-Fos in TPA-treated mouse skin was markedly attenuated by LY294002 as assessed by immunoblot (Fig. 5D, top) and immunohistochemical (Fig. 5D, bottom) analyses. Moreover, there was pronounced suppression of TPA-induced COX-2 expression in mouse skin following cotreatment with LY294002 as determined by immunoblot (Fig. 5E, left; Supplementary Fig. S1D) and immunohistochemical (Fig. 5E, right; Supplementary Fig. S1E) analyses.

DATS inhibited DMBA-initiated and TPA-promoted mouse skin tumorigenesis. The inhibitory effects of DATS on TPA-induced COX-2 expression prompted us to investigate the effect of this organosulfur compound on mouse skin tumor promotion. The onset of papillomagenesis in DMBA-initiated mouse skin occurred 6 weeks after TPA treatment, which resulted in a 100% incidence (Fig. 6A) with an average of 21.89 ± 1.16 papillomas per mouse at the 20th week (Fig. 6B). Although DATS (5 μmol) did not affect the tumor incidence, it reduced the multiplicity of skin tumors by 25.63%. Pretreatment with the higher dose (25 μmol) of DATS reduced both the incidence (Fig. 6A) and the multiplicity (Fig. 6B) of papillomas by 22.22% and 71.08%, respectively.

Discussion

The discovery of intracellular signaling pathways involved in aberrant COX-2 expression and their modulation by dietary phytochemicals provided one of the rational approaches for molecular target-based cancer chemoprevention (7, 21). Garlic has been used as a food additive since the prehistoric time. The oil-soluble fraction of garlic contains organosulfur compounds, which possess chemopreventive properties (16, 17). Among the organosulfur compounds, DATS bearing three sulfur atoms and two allyl moieties exhibits the most potent chemopreventive and anticarcinogenic activities (18, 22–25). In the present study, we examined the anti-inflammatory and antitumor-promoting effects of DATS in TPA-stimulated mouse skin with special focus on its underlying molecular mechanisms. We initially assessed the effect of DATS, at different dose ranges, on TPA-induced COX-2 expression in mouse skin. Based on our preliminary data, we selected 5 or 25 μmol DATS as suitable doses for assessing its anti-inflammatory and antitumor-promoting activities.

Because aberrant expression of COX-2 is causally linked to tumor promotion (12, 26), the inhibitory effect of DATS on TPA-induced COX-2 expression in mouse skin delineates its anti-inflammatory and antitumor-promoting properties. Our finding is in good agreement with the study by Elango and colleagues (18) who showed that DATS suppressed the constitutive expression of *cox-2* mRNA in HEK-293T cells. The proximal promoter region of *COX-2* gene contains a canonical TATA box and various consensus sequences for interacting with a variety of transcription factors, including NF-κB and AP-1 (13, 20). Although DATS inhibited the activation of AP-1, it barely blocked the DNA binding and nuclear localization of NF-κB in TPA-treated mouse skin.[5] However, DATS has been reported to inhibit NF-κB activation in cultured cells *in vitro* (24). Although it is generally considered that the nuclear translocation and DNA binding of NF-κB are critical events for the induction of NF-κB–dependent gene expression (27), several other

[5] Unpublished observation.

studies have shown that the downregulation of NF-κB DNA binding is not necessarily associated with its reduced transcriptional activity (28, 29). Moreover, the efficient transcriptional activation of NF-κB depends on the phosphorylation of its active subunit p65/RelA (30). Thus, it is worthwhile to further investigate the effects of DATS on the phosphorylation and transcriptional activation of NF-κB in TPA-stimulated mouse skin.

In addition to the inhibition of AP-1 DNA binding, the downregulation of TPA-induced c-Jun and c-Fos expression suggests AP-1 as one of the molecular targets of DATS in attenuating inflammation. Because certain organosulfur compounds have been found to directly interact with free sulfhydryl groups (31), DATS may modify critical cysteine residues present in the DNA binding domains of c-Jun and c-Fos, thereby inactivating AP-1.

It has been reported that the activation of AP-1 and expression of COX-2 in TPA-treated mouse skin are regulated by various upstream kinases, including p38 MAPK (9) and JNK (14). In accordance with our previous report (14), the present study further confirmed the role of JNK in regulating AP-1 activation and COX-2 expression in mouse skin treated with TPA. Although DATS failed to modulate TPA-induced p38 MAPK activation (data not shown), the compound significantly attenuated the phosphorylation and the catalytic activity of JNK in TPA-stimulated mouse skin. In contrast, DATS induces apoptosis in various cancer cells through upregulation of JNK (32, 33).

Recent reports have shown that Akt, another upstream kinase, regulates COX-2 expression in various cells in culture and in animal studies (34, 35). The significant decrease in TPA-induced COX-2 expression in female ICR mouse skin treated with LY294002 agrees with our previous study showing that pharmacologic inhibition of Akt abrogated TPA-induced COX-2 expression in male HR-1 hairless mouse skin (15). Our findings that the pharmacologic inhibition of Akt abrogated the DNA binding of AP-1, the expression of c-Jun and c-Fos, and the level of COX-2 suggest that Akt functions as an upstream signaling molecule to activate AP-1 and induce COX-2 in TPA-stimulated mouse skin. The inhibition of Akt-mediated phosphorylation of c-Jun in TPA-treated mouse skin by DATS, therefore, supports the notion that the compound inhibits TPA-induced AP-1 activation and COX-2 expression in mouse skin by blocking the Akt signaling. DATS also induced apoptosis in human prostate cancer PC-3 and DU-145 cells through inactivation of Akt (36). Therefore, Akt may act as a potential upstream target for antiproliferative as well as anti-inflammatory and antitumor-promoting activities of DATS.

In the present study, SP600125 and LY294002 were applied to mouse skin following a pretreatment and cotreatment protocol, respectively. According to our previous studies, pretreatment with SP600125 (14), but not with LY294002 (37), significantly attenuated TPA-induced COX-2 expression in mouse skin. We therefore examined if cotreatment with LY294002 may have any effect on TPA-induced AP-1 activation and COX-2 expression. We found that cotreatment with LY294002 not only downregulated Akt phosphorylation but also attenuated the activity of Akt kinase, with subsequent inhibition of AP-1 activation and COX-2 expression in TPA-stimulated mouse skin.

Several studies have shown the involvement of Akt (38, 39) and JNK (14, 40) in TPA-induced AP-1 activation. Our findings that JNK and Akt regulate TPA-induced AP-1 activation in mouse skin *in vivo* and that DATS inhibits both JNK- and Akt-mediated AP-1 activation suggest a possible cross talk between the JNK and Akt signaling pathways in TPA-treated mouse skin. Whereas JNK has been reported to act downstream of Akt (41), our study shows no such inhibitory effect of LY294002 or SP600125 on the phosphorylation of JNK or Akt, respectively (data not shown), suggesting that TPA-induced JNK or Akt signaling converges independently on the downstream transcription factor AP-1 in mouse skin. In line with our observation, Beales and Ogunwobi (42) showed that pharmacologic inhibition of either JNK or Akt failed to inhibit the phosphorylation of Akt or JNK, respectively, in glycine-extended gastrin-stimulated human colon cancer (HT-29) cells.

The inhibition of COX-2 expression or activity is critical for not only alleviating inflammation but also preventing tumor promotion (4, 21). Thus, the inhibitory effects of DATS on TPA-induced COX-2 expression may account for its antitumor-promoting potential in mouse skin *in vivo*. The significant decrease in the incidence and the multiplicity of papillomas in DMBA-initiated and TPA-promoted mouse skin suggest DATS as a potential cancer chemopreventive agent. In conclusion, DATS suppressed TPA-induced expression of COX-2 by inactivating AP-1 via blockade of upstream JNK and Akt signaling pathways, which provides a mechanistic basis of anti-inflammatory and antitumor-promoting activities of DATS in mouse skin *in vivo*.

Disclosure of Potential Conflicts of Interest

No potential conflicts of interest were disclosed.

Grant Support

21C Frontier Functional Human Genome Project grant FG07-21-21 and National Research Foundation, Ministry of Education, Science and Technology, Republic of Korea ERC grant R11-2007-107-01002-0.

The costs of publication of this article were defrayed in part by the payment of page charges. This article must therefore be hereby marked *advertisement* in accordance with 18 U.S.C. Section 1734 solely to indicate this fact.

Received 09/24/2009; revised 12/01/2009; accepted 12/08/2009; published OnlineFirst 02/23/2010.

References

1. Coussens LM, Werb Z. Inflammation and cancer. Nature 2002;420:860–7.
2. Kundu JK, Surh Y-J. Inflammation: gearing the journey to cancer. Mutat Res 2008;659:15–30.
3. Surh Y-J, Kundu JK. Cancer preventive phytochemicals as speed breakers in inflammatory signaling involved in aberrant COX-2 expression. Curr Cancer Drug Targets 2007;7:447–58.
4. Chun K-S, Surh Y-J. Signal transduction pathways regulating

cyclooxygenase-2 expression: potential molecular targets for chemoprevention. Biochem Pharmacol 2004;68:1089–100.
5. Muller-Decker K, Neufang G, Berger I, Neumann M, Marks F, Furstenberger G. Transgenic cyclooxygenase-2 overexpression sensitizes mouse skin for carcinogenesis. Proc Natl Acad Sci U S A 2002;99:12483–8.
6. Tiano HF, Loftin CD, Akunda J, et al. Deficiency of either cyclooxygenase (COX)-1 or COX-2 alters epidermal differentiation and reduces mouse skin tumorigenesis. Cancer Res 2002;62:3395–401.
7. Surh Y-J, Kundu JK. Signal transduction network leading to COX-2 induction: a road map in search of cancer chemopreventives. Arch Pharm Res 2005;28:1–15.
8. Chun KS, Keum YS, Han SS, Song YS, Kim SH, Surh Y-J. Curcumin inhibits phorbol ester-induced expression of cyclooxygenase-2 in mouse skin through suppression of extracellular signal-regulated kinase activity and NF-κB activation. Carcinogenesis 2003;24:1515–24.
9. Chun KS, Kim SH, Song YS, Surh Y-J. Celecoxib inhibits phorbol ester-induced expression of COX-2 and activation of AP-1 and p38 MAP kinase in mouse skin. Carcinogenesis 2004;25:713–22.
10. Kim SO, Kundu JK, Shin YK, et al. [6]-Gingerol inhibits COX-2 expression by blocking the activation of p38 MAP kinase and NF-κB in phorbol ester-stimulated mouse skin. Oncogene 2005;24:2558–67.
11. Kundu JK, Shin YK, Kim SH, Surh Y-J. Resveratrol inhibits phorbol ester-induced expression of COX-2 and activation of NF-κB in mouse skin by blocking IκB kinase activity. Carcinogenesis 2006;27:1465–74.
12. Kundu JK, Shin YK, Surh Y-J. Resveratrol modulates phorbol ester-induced pro-inflammatory signal transduction pathways in mouse skin *in vivo*: NF-κB and AP-1 as prime targets. Biochem Pharmacol 2006;72:1506–15.
13. Kang YJ, Wingerd BA, Arakawa T, Smith WL. Cyclooxygenase-2 gene transcription in a macrophage model of inflammation. J Immunol 2006;177:8111–22.
14. Lee JC, Kundu JK, Hwang DM, Na HK, Surh Y-J. Humulone inhibits phorbol ester-induced COX-2 expression in mouse skin by blocking activation of NF-κB and AP-1: IκB kinase and c-Jun-N-terminal kinase as respective potential upstream targets. Carcinogenesis 2007;28:1491–8.
15. Hwang DM, Kundu JK, Shin JW, Lee JC, Lee HJ, Surh Y-J. *cis-9, trans*-11-conjugated linoleic acid down-regulates phorbol ester-induced NF-κB activation and subsequent COX-2 expression in hairless mouse skin by targeting IκB kinase and PI3K-Akt. Carcinogenesis 2007;28:363–71.
16. Powolny AA, Singh SV. Multitargeted prevention and therapy of cancer by diallyl trisulfide and related Allium vegetable-derived organosulfur compounds. Cancer Lett 2008;269:305–14.
17. Shukla Y, Kalra N. Cancer chemoprevention with garlic and its constituents. Cancer Lett 2007;247:167–81.
18. Elango EM, Asita H, Nidhi G, Seema P, Banerji A, Kuriakose MA. Inhibition of cyclooxygenase-2 by diallyl sulfides (DAS) in HEK 293T cells. J Appl Genet 2004;45:469–71.
19. Dwivedi C, Rohlfs S, Jarvis D, Engineer FN. Chemoprevention of chemically induced skin tumor development by diallyl sulfide and diallyl disulfide. Pharm Res 1992;9:1668–70.
20. Ramsay RG, Ciznadija D, Vanevski M, Mantamadiotis T. Transcriptional regulation of cyclo-oxygenase expression: three pillars of control. Int J Immunopathol Pharmacol 2003;16:59–67.
21. Surh Y-J. Cancer chemoprevention with dietary phytochemicals. Nat Rev Cancer 2003;3:768–80.
22. Fukao T, Hosono T, Misawa S, Seki T, Ariga T. The effects of allyl sulfides on the induction of phase II detoxification enzymes and liver injury by carbon tetrachloride. Food Chem Toxicol 2004;42:743–9.
23. Jakubikova J, Sedlak J. Garlic-derived organosulfides induce cytotoxicity, apoptosis, cell cycle arrest and oxidative stress in human colon carcinoma cell lines. Neoplasma 2006;53:191–9.
24. Liu KL, Chen HW, Wang RY, Lei YP, Sheen LY, Lii CK. DATS reduces LPS-induced iNOS expression, NO production, oxidative stress, and NF-κB activation in RAW 264.7 macrophages. J Agric Food Chem 2006;54:3472–8.
25. Wu CC, Sheen LY, Chen HW, Kuo WW, Tsai SJ, Lii CK. Differential effects of garlic oil and its three major organosulfur components on the hepatic detoxification system in rats. J Agric Food Chem 2002;50:378–83.
26. Dannenberg AJ, Altorki NK, Boyle JO, et al. Cyclooxygenase 2: a pharmacological target for the prevention of cancer. Lancet Oncol 2001;2:544–51.
27. Baldwin AS, Jr. The NF-κB and IκB proteins: new discoveries and insights. Annu Rev Immunol 1996;14:649–83.
28. Harnish DC, Scicchitano MS, Adelman SJ, Lyttle CR, Karathanasis SK. The role of CBP in estrogen receptor cross-talk with nuclear factor-κB in HepG2 cells. Endocrinology 2000;141:3403–11.
29. Takahashi N, Tetsuka T, Uranishi H, Okamoto T. Inhibition of the NF-κB transcriptional activity by protein kinase A. Eur J Biochem 2002;269:4559–65.
30. Ghosh S, Karin M. Missing pieces in the NF-κB puzzle. Cell 2002;109:S81–96.
31. Bianchini F, Vainio H. Allium vegetables and organosulfur compounds: do they help prevent cancer? Environ Health Perspect 2001;109:893–902.
32. Wu XJ, Hu Y, Lamy E, Mersch-Sundermann V. Apoptosis induction in human lung adenocarcinoma cells by oil-soluble allyl sulfides: triggers, pathways, and modulators. Environ Mol Mutagen 2009;50:266–75.
33. Xiao D, Choi S, Johnson DE, et al. Diallyl trisulfide-induced apoptosis in human prostate cancer cells involves c-Jun N-terminal kinase and extracellular-signal regulated kinase-mediated phosphorylation of Bcl-2. Oncogene 2004;23:5594–606.
34. Bachelor MA, Cooper SJ, Sikorski ET, Bowden GT. Inhibition of p38 mitogen-activated protein kinase and phosphatidylinositol 3-kinase decreases UVB-induced activator protein-1 and cyclooxygenase-2 in a SKH-1 hairless mouse model. Mol Cancer Res 2005;3:90–9.
35. Liao SL, Ou YC, Chen SY, Chiang AN, Chen CJ. Induction of cyclooxygenase-2 expression by manganese in cultured astrocytes. Neurochem Int 2007;50:905–15.
36. Xiao D, Singh SV. Diallyl trisulfide, a constituent of processed garlic, inactivates Akt to trigger mitochondrial translocation of BAD and caspase-mediated apoptosis in human prostate cancer cells. Carcinogenesis 2006;27:533–40.
37. Lee JY, Shin JW, Chun KS, et al. Antitumor promotional effects of a novel intestinal bacterial metabolite (IH-901) derived from the protopanaxadiol-type ginsenosides in mouse skin. Carcinogenesis 2005;26:359–67.
38. Kikuchi J, Kinoshita I, Shimizu Y, et al. Simultaneous blockade of AP-1 and phosphatidylinositol 3-kinase pathway in non-small cell lung cancer cells. Br J Cancer 2008;99:2013–9.
39. Ma C, Bower KA, Lin H, et al. The role of epidermal growth factor receptor in ethanol-mediated inhibition of activator protein-1 transactivation. Biochem Pharmacol 2005;69:1785–94.
40. Yu X, Luo A, Zhou C, et al. Differentiation-associated genes regulated by TPA-induced c-Jun expression via a PKC/JNK pathway in KYSE450 cells. Biochem Biophys Res Commun 2006;342:286–92.
41. Funakoshi-Tago M, Tago K, Sonoda Y, Tominaga S, Kasahara T. TRAF6 and C-SRC induce synergistic AP-1 activation via PI3-kinase-AKT-JNK pathway. Eur J Biochem 2003;270:1257–68.
42. Beales IL, Ogunwobi O. Glycine-extended gastrin inhibits apoptosis in colon cancer cells via separate activation of Akt and JNK pathways. Mol Cell Endocrinol 2006;247:140–9.